AMERICAN SOCIETY FOR MICROBIOLOGY | Infection and Immunity

Biological Activities of Uric Acid in Infection Due to Enteropathogenic and Shiga-Toxigenic *Escherichia coli*

John K. Crane, Jacqueline E. Broome, Agnieszka Lis

Department of Medicine, Division of Infectious Diseases, University at Buffalo, Buffalo, New York, USA

In previous work, we identified xanthine oxidase (XO) as an important enzyme in the interaction between the host and enteropathogenic *Escherichia coli* (EPEC) and Shiga-toxigenic *E. coli* (STEC). Many of the biological effects of XO were due to the hydrogen peroxide produced by the enzyme. We wondered, however, if uric acid generated by XO also had biological effects in the gastrointestinal tract. Uric acid triggered inflammatory responses in the gut, including increased submucosal edema and release of extracellular DNA from host cells. While uric acid alone was unable to trigger a chloride secretory response in intestinal monolayers, it did potentiate the secretory response to cyclic AMP agonists. Uric acid crystals were formed *in vivo* in the lumen of the gut in response to EPEC and STEC infections. While trying to visualize uric acid crystals formed during EPEC and STEC infections, we noticed that uric acid crystals became enmeshed in the neutrophilic extracellular traps (NETs) produced from host cells in response to bacteria in cultured cell systems and in the intestine *in vivo*. Uric acid levels in the gut lumen increased in response to exogenous DNA, and these increases were enhanced by the actions of DNase I. Interestingly, addition of DNase I reduced the numbers of EPEC bacteria recovered after a 20-h infection and protected against EPEC-induced histologic damage.

Xanthine oxidase (XO), also known as xanthine oxidoreductase (XOR), has been hailed as an important host defense against enteric pathogens for decades (1, 2). In a recent study, however, we found that XO could have deleterious as well as beneficial effects in the context of infection with Shiga-toxigenic *Escherichia coli* (STEC) (3). One of the deleterious effects of XO was its ability to induce production of the Shiga toxins (Stx) from STEC bacteria. Low to intermediate amounts of XO activity generated enough H_2O_2 to induce Stx but not enough to actually kill STEC or enteropathogenic *E. coli* (EPEC) bacteria, resulting in an "uncanny valley" of worsened disease outcome.

In addition to H_2O_2, XO also generates uric acid as a product. While uric acid used to be viewed as an inert waste product of purine metabolism, recent advances have highlighted the biological roles of uric acid in inflammation and innate immunity (4, 5). Although monosodium urate (MSU) is the technically more accurate term, we will use "uric acid" here, since the latter term is deeply entrenched in the biomedical literature. In a previous study, we found that uric acid crystals were formed *in vivo* in response to EPEC and STEC infection in the lumen of the gastrointestinal (GI) tract (6). In the present study, we focused on determining the biological effects of uric acid, as opposed to H_2O_2, produced by XO. We investigated the effects of uric acid on inflammatory responses, as well as secretory responses, in intestinal tissues and found that uric acid acted as a potentiator or modulator of proinflammatory or prosecretory agonists and that its crystals became enmeshed in the DNA of neutrophilic extracellular traps (NETs). Manipulation of the formation of NETs using DNase and uricase altered the outcome of EPEC infection in rabbit ligated intestinal loops *in vivo*.

MATERIALS AND METHODS

Materials. fMet-Leu-Phe, forskolin, uric acid, and Hoechst 22358 dye were from Sigma-Aldrich; uric acid was dissolved in 50 mM sodium borate buffer, pH 8.5, in which it remains in solution for about 1 week, after which precipitation is observed. Phorbol myristate acetate (PMA) was from LC Laboratories, Woburn, MA. Sytox Orange was from the Molecular Probes Division of Thermo-Fisher. DNase I, micrococcal nuclease, and uricase were from Worthington Biochemicals, Lakewood, NJ. Uricase is also known as urate oxidase. Guanylin was from Bachem Corp., Torrance, CA.

Bacterial strains used. The bacterial strains used are described in Table 1. We included pathogenic *E. coli* strains and not just laboratory strains, since pathogenic strains may have better ability to resist killing by host defenses, including DNA NETs.

Interleukin 1β assay. Rabbit interleukin 1β (IL-1β) production was assayed using a kit from Cloud-Clone Corp., Houston, TX.

HL-60 cells. HL-60 cells, a human promyelocytic leukemia line, were obtained from the ATCC, Manassas, VA, and were maintained in Dulbecco's modified Eagle's medium (DMEM)–F-12 with 18 mM $NaHCO_3$ and 7.5% fetal bovine serum. The HL-60 cells were induced to differentiate into neutrophil-like cells by treatment with 1.1% dimethyl sulfoxide (DMSO) plus 10 μM all-*trans*-retinoic acid (ATRA) for 48 h. For some experiments testing chemotaxis or ATP release, HL-60 cells were used without chemically induced differentiation.

Isolation of rabbit peripheral blood leukocytes (PBLs). Rabbit blood obtained by ear vein was subjected to the ammonium chloride lysis method of Tait et al. (7) to obtain leukocytes.

Ussing chamber measurements using T84 cells. T84 cells, a secretion-competent colon cell line, were grown to confluence in Snap-Well inserts (Corning Costar) and used for measurement of chloride secretion in an Ussing chamber as described previously (3, 8).

Chemotaxis assay. The ability of uric acid to trigger chemotaxis of HL-60 cells was tested using the Trevigen Cultrex cell migration assay

Received 11 November 2015 Returned for modification 8 December 2015
Accepted 14 January 2016

Accepted manuscript posted online 19 January 2016

Citation Crane JK, Broome JE, Lis A. 2016. Biological activities of uric acid in infection due to enteropathogenic and Shiga-toxigenic *Escherichia coli*. Infect Immun 84:976–988. doi:10.1128/IAI.01389-15.

Editor: V. B. Young

Address correspondence to John K. Crane, jcrane@buffalo.edu.

Supplemental material for this article may be found at http://dx.doi.org/10.1128/IAI.01389-15.

TABLE 1 Bacterial strains used

Strain	Serotype	Description	Reference(s) or source
E2348/69	O127:H7	Typical human EPEC	43, 44
E22	O103:H2	Rabbit EPEC	45
E22-stx2	O103:H2	Rabbit STEC created from E22	46, 47
DH5α-(pGFP-UV)		Fluorescently (GFP) tagged version of DH5α (catalog no. 632312)	Clontech Laboratories (now TaKaRa Clontech)

(Trevigen, Gaithersburg, MD). This assay uses 24-well or 96-well plate inserts with an 8-μm-pore-size membrane to measure cell migration from the upper to the lower chamber. In our initial experiments, the cell wells were not coated with any protein or DNA, and 50,000 HL-60 cells were placed into the upper chambers of 96-well plates according to the instructions. In later experiments, we used the larger, 24-well plate inserts and coated the wells with 100 μl of 100 μg/ml DNA, which was allowed to dry; the number of HL-60 cells was increased to 400,000 per chamber in the larger wells. The cells that migrated were counted using a TC20 cell counter (Bio-Rad Laboratories, Hercules, CA).

DNA binding dyes for extracellular DNA NETs. Sytox Orange, a cell-impermeant DNA binding dye, was obtained from the Molecular Probes division of Thermo-Fisher and used at a concentration of 5 μM to label extracellular DNA released from cells. Fluorescent signal was measured using a 96-well-plate fluorescence plate reader. Hoechst dye 22358 was prepared as a stock in DMSO and then used at a final concentration of 5 μg/ml to stain DNA for fluorescence microscopy. Sytox Orange was used at 10 μM in some microscopy experiments, as well.

ATP release. ATP was measured in the sterile filtrates of HL-60 cells using the Sigma Luciferase ATP assay kit as previously described (9). We used an ATP regenerating system consisting of 100 μg/ml creatine kinase and 15 mM phosphocreatine to prevent destruction of extracellular ATP during the 2-h assay.

Polarization microscopy for birefringent crystals was performed as described previously (6).

Rabbit intestinal loop infection experiments. Animal work was approved by the IACUC of the University at Buffalo. Infection of 10-cm ileal loops in New Zealand White rabbits was done using rabbit EPEC strain E22 or rabbit STEC strain E22-stx2 and an inoculum of 4×10^8 CFU per intestinal loop, as described previously (3). Submucosal width was measured on the digital images using the measurement function built into the QCapture Suite Plus software (version 3.1.3) for the Macintosh computer after calibrating using 15-μm sizing beads.

Data analysis and statistics. The error bars shown in all graphs indicate standard deviations (SD). Comparisons involving multiple groups were done by analysis of variance (ANOVA) using Dunnett's test for multiple comparisons. Comparison of 2 groups was by *t* test, and the level of significance was a *P* value of ≤0.05.

RESULTS

Our previous work had indicated that uric acid had proinflammatory effects in the GI tract and that it had the ability to trigger an increase in influx of polymorphonuclear cells into the gut lumen (at 600 μM), as measured by a myeloperoxidase (MPO) assay (6). To determine if uric acid acted as a true chemoattractant, we studied the effects of uric acid on the migration of HL-60 cells and rabbit PBLs in a modified Boyden chamber. As shown in Fig. 1A, uric acid at 200 to 600 μM failed to cause an increase in migration of HL-60 cells toward the uric acid. However, these experiments were hampered by a very high rate of migration of HL-60 cells without any chemotactic stimulus (Fig. 1A to C, *y* axes). To attempt to reduce the basal level of HL-60 cell migration, we coated the membranes with DNA and repeated our measurements. DNA significantly reduced the migration of HL-60 cells compared to uncoated wells (Fig. 1B and C). With the basal level of migration reduced, the chemoattractant peptide fMet-Leu-Phe significantly increased the number of cells that moved by chemotaxis to the lower chamber (Fig. 1B). Exogenous DNase I, as expected, also increased the cell migration (Fig. 1B). However, under these optimized conditions, uric acid still did not trigger chemotaxis toward itself, even when the concentration of uric acid was increased to 1,000 μM (Fig. 1C). Similar negative results were also observed with HL-60 cells that were induced to differentiate using DMSO and retinoic acid and with rabbit PBLs (data not shown). Therefore, whether we used wells that were coated or uncoated or cells that were differentiated or left undifferentiated, uric acid's effects on leukocytes did not include the ability to recruit leukocytes from a distance, as a true chemoattractant would do.

Since exogenous DNA impeded the ability of HL-60 cells to cross a semipermeable membrane (Fig. 1B and C), we tested whether uric acid might have a similar effect. Coating migration wells with uric acid reduced the migration of HL-60 cells (Fig. 1D), and the effects of uric acid were additive with those of DNA (Fig. 1D). Therefore, while uric acid does not function as a chemoattractant, it can impede the ability of cells to cross a membrane and therefore might be able to trap leukocytes that are attracted into the vicinity by other stimuli.

Some of the inflammatory effects of uric acid are mediated by its ability to signal via the NLRP3 inflammasome and thereby induce the release of IL-1β. We tested uric acid's ability to stimulate IL-1β release from rabbit PBLs. IL-1β levels, as measured by enzyme immunoassay (EIA) in this system, were at or near the lower limit of detection in the assay, about 1.4 pg/ml (Fig. 1E). Phorbol myristate acetate (PMA) (0.1 μM) stimulated IL-1β in the rabbit cells, but the effects of uric acid did not reach statistical significance. Despite the low levels of IL-1β we observed, the ability of uric acid to signal via the NLRP3 inflammasome pathway is well documented by previous studies (5, 10). Rabbits have not been popular subjects in studies of uric acid actions in recent years, and older studies used bioassays, rather than EIA, to measure IL-1β activity (11). Therefore, there is no recent literature against which to compare our results with rabbit leukocytes and IL-1β.

While testing for the ability of uric acid to increase MPO activity in rabbit intestinal segments, we also noted another effect of uric acid: its ability to trigger an increase in submucosal edema *in vivo*. Figure 1F and H show that 600 μM uric acid increased submucosal edema to a degree equivalent to that caused by 3,500 pg/ml Stx2. Figure 1G, in contrast, shows the normal submucosal space in an untreated control rabbit intestinal loop. Although marked submucosal edema is observed in human cases of STEC infection (12), the mechanism of this edema response in the intestine has not been well studied, since it is not observed in most mouse models of STEC infection (13) and is also not observed when Stx is injected parenterally. Unfortunately, the mechanisms

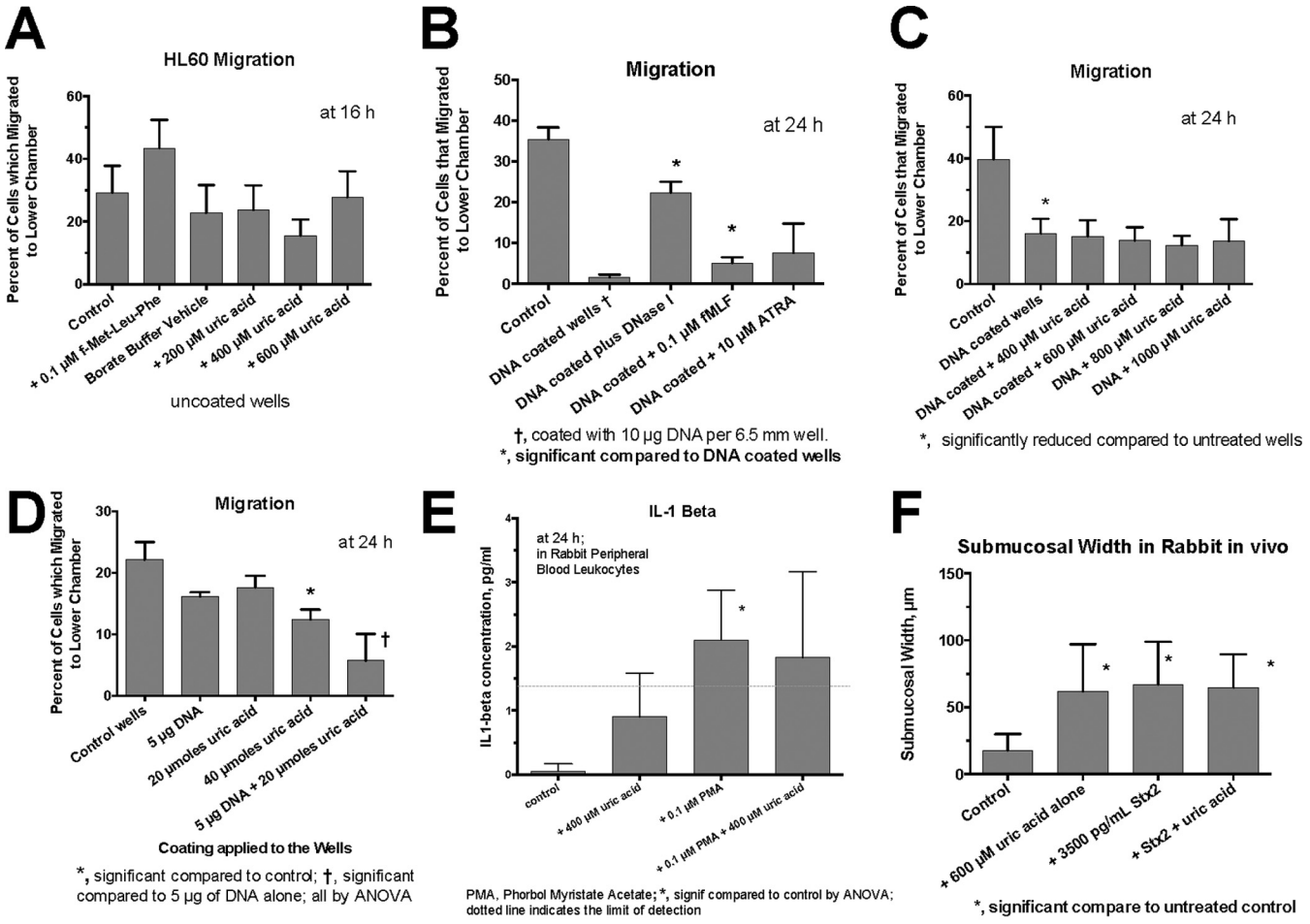

FIG 1 Effects of uric acid on indices of inflammation. (A to D) Effect of uric acid on HL-60 cell chemotaxis or spontaneous migration across an 8-μm-pore-size membrane from the upper to the lower chamber in Trevigen cell migration plates. (A) Lack of effect of uric acid on migration of HL-60 cells using uncoated membranes. (B) Coating the cell wells with 10 μg of DNA reduced the spontaneous migration of HL-60 cells across the membrane. In the presence of DNA, both fMet-Leu-Phe and DNase I (100 U/ml) increased the migration of HL-60 cells across the membrane. (C) In wells coated with 10 μg DNA, uric acid added to the lower chamber still failed to trigger chemotaxis across the membrane. (D) Effect of coating the migration wells with either DNA or uric acid or both. (E) Effects of PMA with or without uric acid on IL-1β production from rabbit peripheral blood leukocytes. (F to H) Effects of uric acid with or without Stx2 toxin on submucosal width in rabbit intestinal segments. (G and H) Normal control intestine (G) and rabbit intestinal loop treated with 600 μM uric acid alone (H). The double-headed arrows show the submucosal space; the arrow in panel H indicates a submucosal width of 74 μm. Magnification, ×100 (G and H). The error bars indicate SD.

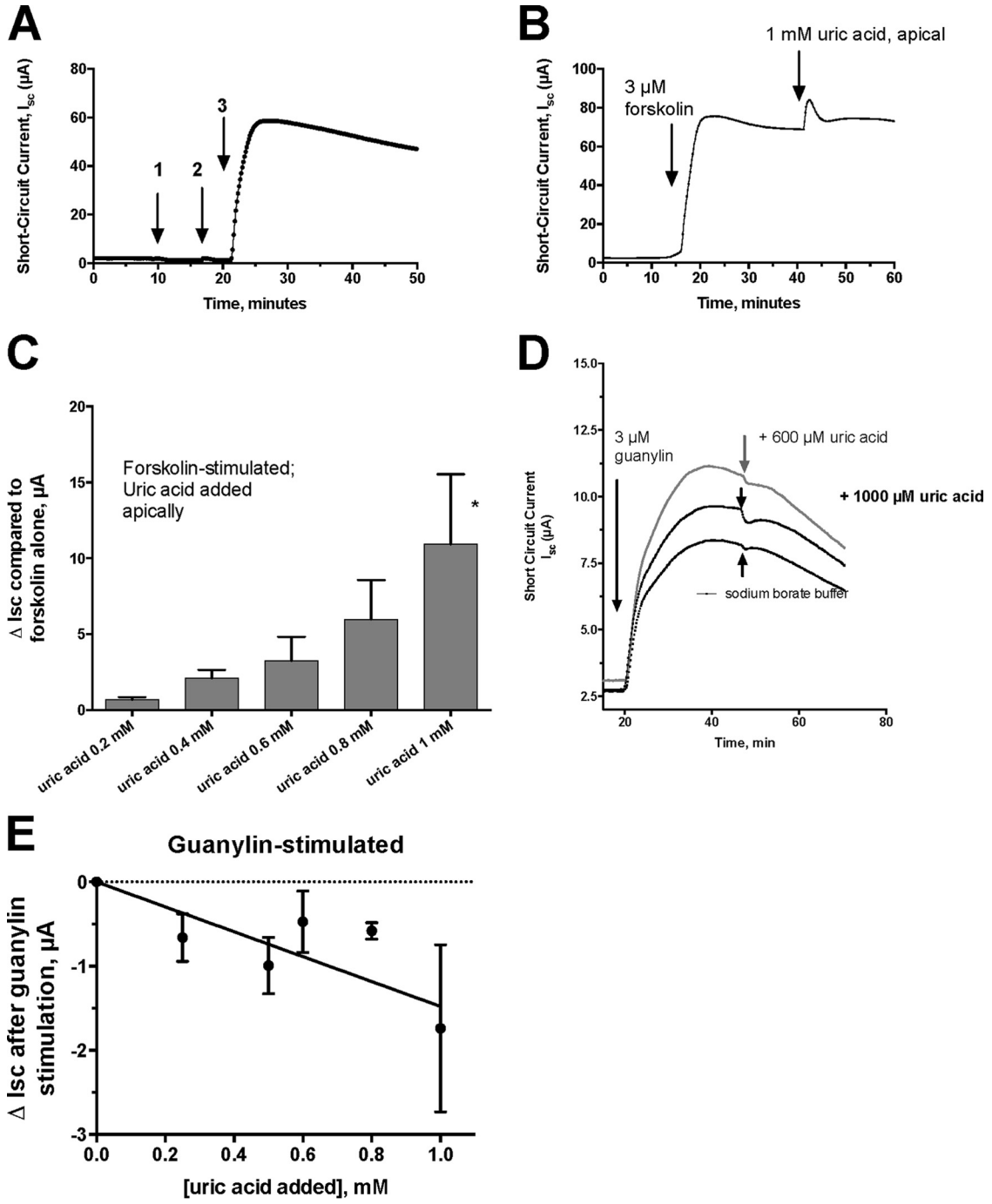

FIG 2 Effect of uric acid on chloride secretion in T84 cells in an Ussing chamber. All the tracings represent short-circuit current (I_{sc}) tracings expressed in microamperes. (A) Lack of effect of adding 1 mM uric acid on the apical side (arrow 1) or on the basolateral side (arrow 2) of the monolayer. Arrow 3 shows that the tissue is still competent in secretion and responsive to 3 μM forskolin. (B) Additive effect of uric acid on secretion induced by forskolin. Forskolin (3 μM) was added first, and then uric acid was added apically, as indicated by the arrows. (C) Dose response of apical uric acid on ΔI_{sc}, defined as the increase in I_{sc} after adding uric acid. Each bar represents the mean and SD of 3 tracings. *, significantly greater than result with forskolin alone. (D) Effect of apical uric acid on I_{sc} triggered by 3 μM guanylin, a cyclic GMP agonist. The top curve shows the response to 600 μM uric acid; the middle curve shows a small inhibitory effect of 1 mM uric acid, and the bottom curve shows the lack of effect of the sodium borate buffer. (E) Dose-dependent inhibition of guanylin-induced I_{sc} by uric acid. Each point represents the mean ± SD of 3 tracings.

of both Stx-induced mucosal edema and uric acid-induced submucosal edema remain unknown.

Our laboratory has been interested in how EPEC and STEC infections trigger intestinal-fluid secretion that results in diarrhea. We discovered that the hydrogen peroxide produced by XO was able to stimulate a chloride secretory response in intestinal monolayers (3, 14). We investigated if uric acid itself had any effects on intestinal chloride secretion. Figure 2A shows that 1 mM uric acid

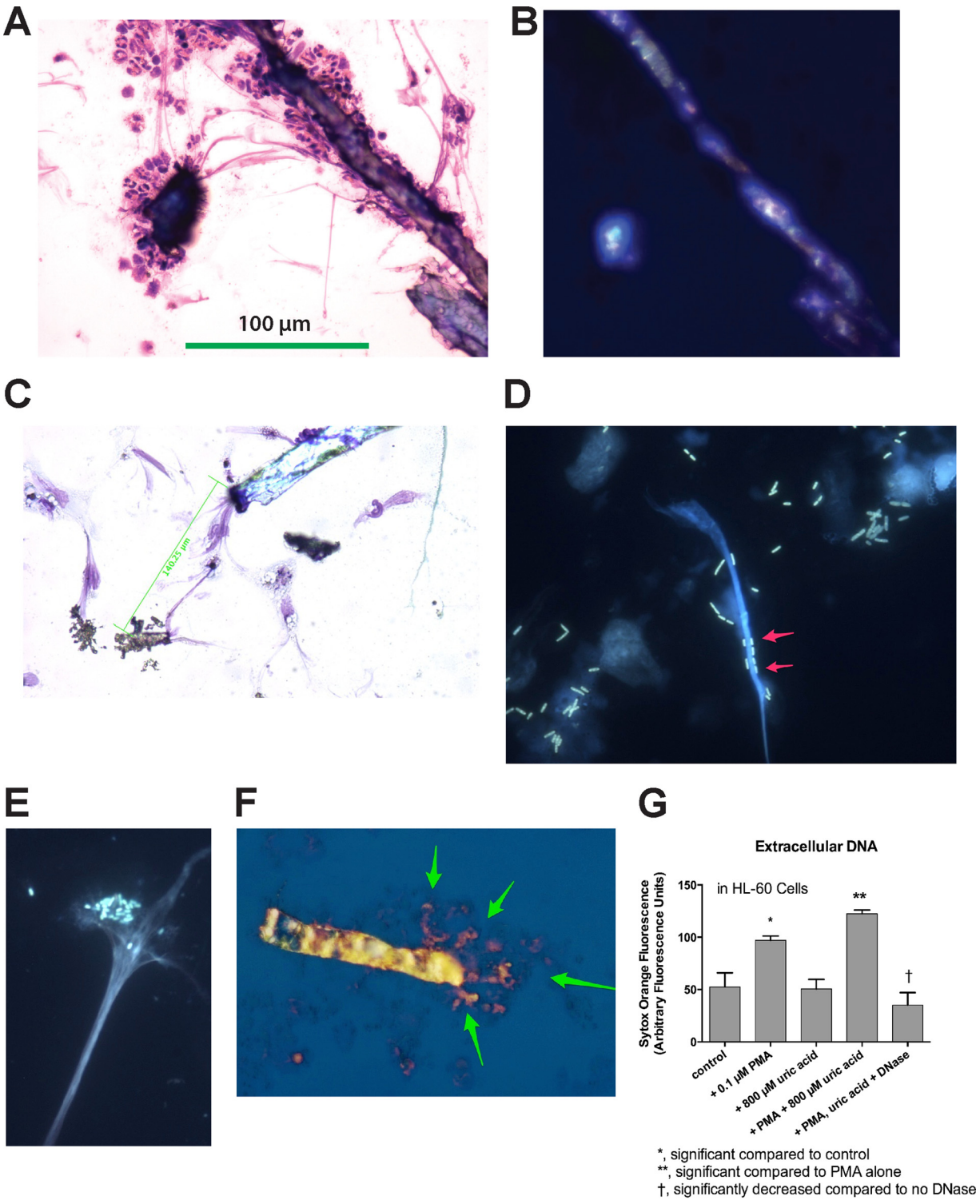

FIG 3 Incorporation of uric acid into DNA NETs. (A, B, and F) Formation of DNA NETs from rabbit peripheral blood leukocytes stimulated with 0.1 μM PMA. (C to E) Images obtained with differentiated HL-60 cells. (A) Bright-field microscopy of PMA-stimulated PBLs showing adherence of leukocytes to crystals and stringy filaments connecting the crystals (three-step stain; magnification, ×100). (B) Polarization microscope image of the same field as in panel A, demonstrating that the crystals show birefringence. The 100-μm scale bar in panel A also applies to panel B. (C) Bright-field microscope image showing that crystals are connected over long distances by stringy filaments, which appear to originate from the nuclei of PMA-treated HL-60 cells. (D) Fluorescent DH5α bacteria expressing green fluorescent protein (GFP) adhere to DNA NETs (arrows) (magnification, ×600; Hoechst stain for DNA). (E) Adherence of human EPEC E2348/69 bacteria to DNA NETs generated from PMA-stimulated HL-60 cells stained with Hoechst dye for DNA. Note that the EPEC bacteria demonstrate their typical localized adherence pattern even when adhering to DNA (magnification, ×600). (F) Merged image showing a birefringent uric acid crystal (photographed by polarization microscopy) superimposed on the same field photographed under fluorescence, with staining using 10 μM Sytox Orange. The orange-stained DNA seems to emanate from one end of the uric acid crystal (arrows). The uric acid crystal itself is 118 μM in length. (G) Uric acid-induced DNA release from HL-60 cells at 3 h of treatment. The error bars indicate SD.

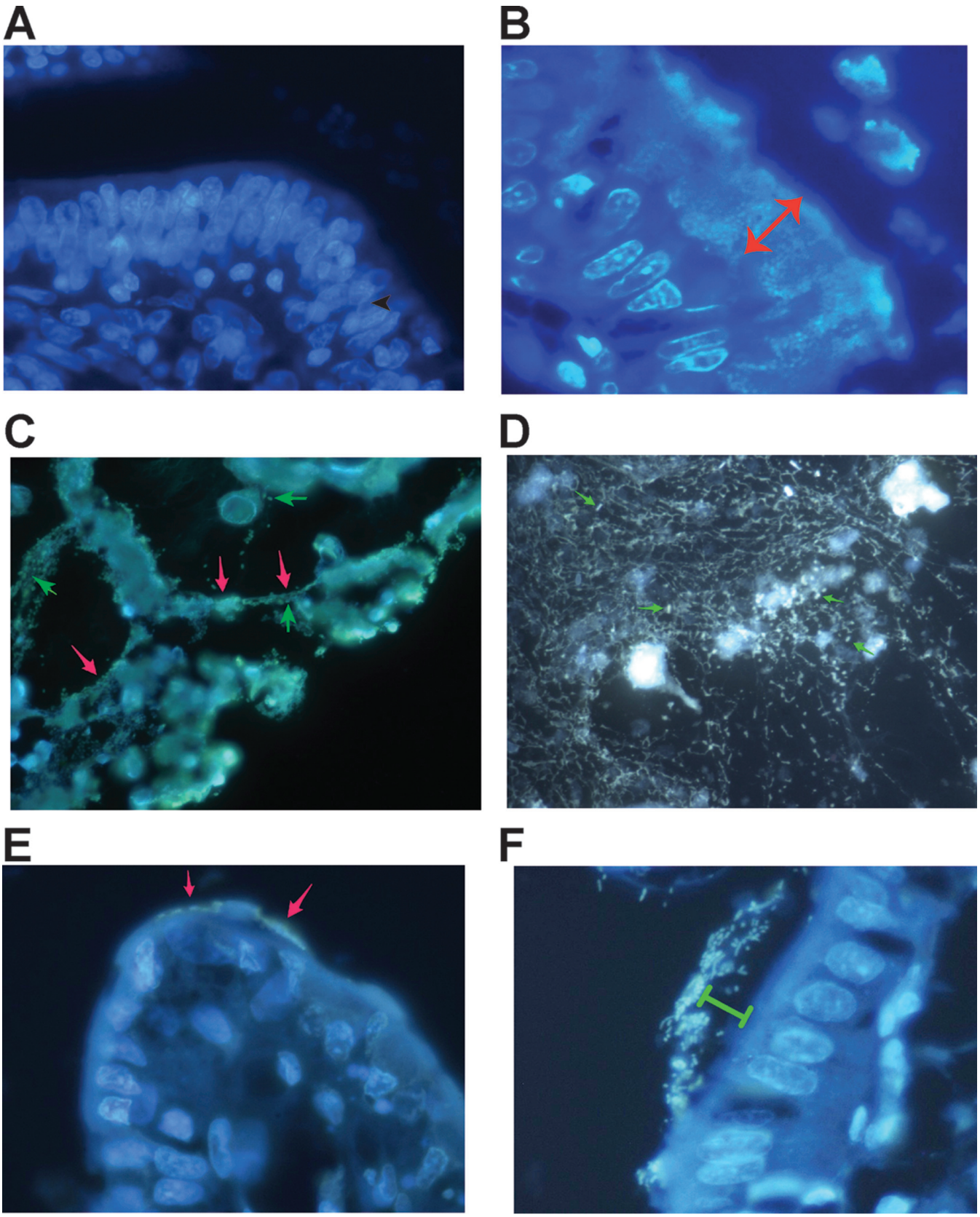

FIG 4 Formation of DNA NETs *in vivo* in the lumen of the GI tract in rabbit. (A) Hoechst stain of the ileum of a healthy uninfected rabbit. The intestinal segment was fixed in formaldehyde, embedded in paraffin, sectioned, and then deparaffinized and stained with 5 μg/ml Hoechst 33258 dye. (B) Hoechst stain of the ileum of a rabbit intestinal segment infected with rabbit STEC strain E22-stx2 for 20 h. The lumen of the gut is at the top right. STEC bacteria are adhering as a thick

had no effect on intestinal chloride secretion if added to the apical side of the monolayer (arrow 1) or to the basolateral side (arrow 2). If the intestinal monolayer was stimulated to secrete using the agonist forskolin, however, then subsequent addition of uric acid did produce an additional increase in the short-circuit current (I_{sc}) (Fig. 2B, right arrow). The increase in I_{sc} (ΔI_{sc}) was dose dependent (Fig. 2C), so that 1 mM uric acid was able to enhance forskolin-induced I_{sc} by 10 μA. Uric acid was also able to enhance I_{sc} when it was added to the basolateral side, but the ΔI_{sc} from basolateral uric acid was only about two-thirds of that observed when uric acid was applied apically (data not shown). Since EPEC and STEC infections cause uric acid release into the intestinal lumen, we believe that the prosecretory effects of uric acid acting from the apical (or lumenal) side are of greater physiological relevance. Uric acid enhanced the secretory effects of cyclic AMP agonists other than forskolin, including adenosine, *N*-ethyl-carboxamidoadenosine (NECA), and dipyridamole (data not shown), in monolayers, as well. However, uric acid did not enhance the chloride secretory response to guanylin, which acts on guanylyl cyclase C to stimulate cyclic GMP in the intestinal cell (Fig. 2D). Instead of enhancing the response to guanylin, uric acid inhibited guanylin-stimulated I_{sc} modestly, but in a dose-dependent manner (Fig. 2E). Our results are the first to show that uric acid can modulate the electrophysiological response to other secretory agonists in the intestine.

Figure 3A and B show that treatment of rabbit PBLs with PMA plus 600 μM uric acid triggered the recruitment of rabbit leukocytes to the uric acid crystals. In addition, the crystals and the PBLs appeared to be linked by a network of long, stringy filaments. Figure 3B shows the same microscope field depicted in Fig. 3A and reveals that the crystals observed in Fig. 3A showed birefringence under polarized light. Uric acid crystals could also be observed in the microscope using bright-field illumination (Fig. 3C) in slides stained with the three-step stain (similar to Wright's stain for blood cells). Uric acid crystals were frequently connected by stringy filaments that appeared to be DNA based on the color of the filaments (lavender, the color of cell nuclei) and the fact that the filaments often emanated from damaged cell nuclei (Fig. 3C). The filaments could be quite long, as indicated by the scale bars in Fig. 3A and C. The images in Fig. 3A to C seem to indicate that the nucleic acid filaments could "organize" the extracellular space by connecting cells, DNA, and crystals over long distances. In order to determine if the filaments observed were indeed DNA, we also stained specimens with DNA binding dyes, such as Hoechst dye and Sytox Orange. Figure 3D and E show that DNA NETs could also be generated from differentiated HL-60 cells by infection with the laboratory *E. coli* strain DH5α-(pGFP-UV) (Fig. 3D), as well as with EPEC bacteria, strain E2348/69 (Fig. 3E). As shown in Fig. 3D, *E. coli* bacteria adhered tightly to the DNA NETs, often lining up along the DNA like boxcars on a railroad track (arrows), but not to the uric acid crystals. We noted that uric acid crystals did not fluoresce after treatment with the DNA binding dyes, except when the uric acid crystals were entangled in DNA. Figure 3F illustrates this with a merged image formed by photographically superimposing 2 images. For Fig. 3F, a uric acid crystal was visualized and photographed by polarization microscopy using visible light. Then, the visible light was turned off, the UV light was turned on, and the same field was photographed again, allowing DNA to be revealed by its orange-red fluorescence from the Sytox Orange. As shown in Fig. 3F, the DNA appears to radiate from one end of the uric acid crystal (arrows). The crystal in Fig. 3F is 118 μm in length, which is much larger than an average human or rabbit cell. Uric acid crystals not only became entangled in DNA NETs, but also appeared to be able to induce the formation of extracellular DNA NETs, as measured by Sytox Orange fluorescence (Fig. 3G). Uric acid-enhanced DNA release was also observed in rabbit peripheral blood leukocytes and in rabbit peritoneal leukocytes in a manner similar to the HL-60 cell results in Fig. 3G (data not shown). The results of Fig. 3G also confirm the results reported by Schorn et al. (15, 16), whose work was reported after we began our study. Our work goes beyond the results of Schorn et al., however, because those researchers did not include any work on microbial pathogens in their studies on uric acid and DNA NETs.

The finding that DNA NETs were formed from rabbit PBLs and HL-60 cells served as the impetus to determine if DNA NETs were formed *in vivo* in the rabbit intestine in response to infection. Figure 4A shows the normal rabbit epithelium of the ileum stained with Hoechst 33258 dye and shows that no bacteria adhering to epithelial cells are visible. Enterocyte nuclei, however, are easily visualized using the Hoechst dye. In contrast, rabbit STEC E22-stx2 adheres strongly to rabbit ileum, forming a biofilm over 20 μm thick (Fig. 4B, double-headed arrow), again visualized using Hoechst dye. The DNA inside bacteria fluoresced so brightly in the STEC biofilm that it was difficult to distinguish if extracellular DNA NETs were also present, although a halo of fluorescence seemed to envelope the STEC-infected cells of the mucosa.

A bit further away from the thickest area of bacterial adherence, in the zone where damaged intestinal cells were being sloughed into the intestinal lumen, it was easier to visualize DNA NETs (Fig. 4C). In Fig. 4C, DNA strands appear to be stretched taut between sloughed cells and cell fragments (red arrows). The intestinal villi and brush border mucosa are at the top in Fig. 4C. Individual EPEC E22 bacteria (green arrows) appear small in the photograph compared to the large scale of the DNA NETs. The DNA NETs formed *in vivo* were not always in the form of linear filaments, as in Fig. 4C, but instead sometimes appeared as a fine, delicate, lacy network, as shown in Fig. 4D. Again, individual EPEC E22 bacteria (Fig. 4D, arrows) were visible trapped in the DNA NETs formed *in vivo*, reminiscent of flies trapped in a spider web. Our observations, as shown in Fig. 4, indicated that DNA NETs were formed *in vivo* during infection with EPEC and STEC alone and without the need to add exogenous uric acid, PMA, or other stimulatory chemicals. The NETs were easily visualized in

biofilm (double-headed arrow, which is 20.8 μm in length). The scale in panel B also applies to panels A, C, and D. (C) DNA NETs formed *in vivo* from rabbit intestine infected with rabbit EPEC strain E22. Cells that are being sloughed into the intestine are connected by DNA strands (red arrows) and surrounded by bacteria. A few individual EPEC bacteria are indicated by green arrows (magnification, ×600). (D) Another field from an intestine infected with EPEC E22 and stained with 10 μg/ml DAPI, showing that the DNA NETs can form a delicate, lacy network and not just linear strands. A few individual EPEC bacteria are again indicated by arrows. (E and F) Effect of DNase I on NETs formed during infection with EPEC E22 (magnification, ×1,000). (E) DNase-treated intestinal loops showed markedly fewer adherent bacteria; the arrows indicate a few E22 bacteria adhering to a villus tip. (F) Remnant bacteria observed in DNase-treated intestinal loops seemed to be adhering "at a distance" rather than in the typical intimate adherence pattern seen in panel B. Green bracket, 8 μm.

cut sections of intestine stained with Hoechst dye (Fig. 4A to C), with DAPI (4′,6-diamidino-2-phenylindole) (Fig. 4D), or with 10 μg/ml ethidium homodimer (data not shown). To our knowledge, our work is the first to show formation of neutrophilic extracellular traps in the intestine in response to an enteric infection.

Although the experiments shown in Fig. 4 indicated that NETs were formed *in vivo* in response to EPEC and STEC infections, this left us with little understanding of the role that NETs, or uric acid, might play in enteric infection. The canonical theory about NETs is that they trap bacteria and enhance the ability of the host to control infection by phagocytosis, antimicrobial peptides, or other means. We attempted to determine the role of NETs using *in vitro* and *in vivo* infection experiments.

Figure S1 in the supplemental material shows the results of adding uricase or DNase I in short-term *in vitro* infection experiments. Figure S1A in the supplemental material shows that, in the presence of uricase, uric acid can generate antibacterial activity. Uricase is also known as urate oxidase and, like XO, generates H_2O_2 as a product of its catalytic activity. In the presence of differentiated, PMA-activated HL-60 cells (see Fig. S1B in the supplemental material), uric acid plus uricase showed antibacterial activity similar to that seen in the absence of leukocytes. We had expected that adding the HL-60 cells would increase the amount of bacterial killing due to the antimicrobial components of these cells, including NADPH oxidase, myeloperoxidase, and the ability to generate NETs (Fig. 3D to F). In addition, we thought that addition of DNase I would impair host defenses (by destroying NETs) and thereby increase bacterial survival, but we were wrong in this prediction, as well (see Fig. S1C in the supplemental material). In contrast, addition of exogenous uricase did reduce survival of EPEC E2348/69 *in vitro*, albeit by a modest 2-fold decrease.

In order to go beyond *in vitro* experiments with cultured HL-60 cells, we sought to determine the roles of NETs and uric acid in the rabbit ligated intestinal loop model. Figure 5A shows that, in contrast to what we observed using HL-60 cells, adding exogenous uricase did not reduce the number of EPEC E22 bacteria recovered from the intestinal segments. Addition of exogenous DNase I, however, did reduce the number of pathogenic bacteria recovered at the end of infection by 1 log unit (Fig. 5B); exogenous micrococcal nuclease had a similar effect but just missed achieving statistical significance (Fig. 5B). These results were the opposite of what we observed in the HL-60 cell experiments (see Fig. S1 in the supplemental material) and the opposite of what one would expect if DNA NETs were acting as an antibacterial host defense. Nevertheless, the findings observed in Fig. 5B were very reproducible and were seen in 6 of 6 intestinal loops (3 of 3 rabbits). In addition to reducing the number of EPEC bacteria recovered, exogenous DNase I also reduced the amount of myeloperoxidase in the intestinal-loop fluid, a measure of neutrophil influx (Fig. 5C). In contrast, addition of exogenous uricase did not reduce the amount of myeloperoxidase induced by EPEC E22 infection (Fig. 5D), but DNase plus uricase did also lower the amount of myeloperoxidase (Fig. 5D). Moreover, addition of DNase provided protection against the tissue damage caused by EPEC E22 infection, as measured by the villus-to-crypt ratio, a measure of villus blunting (Fig. 5E).

Addition of DNase I had another unexpected effect in intestinal loops infected with EPEC E22. In addition to reducing the number of E22 bacteria recovered, exogenous DNase I seemed to increase the number of non-*E. coli* colonies recovered on MacConkey agar (MacConkey agar plus 50 μg/ml nalidixic acid was used for E22). As shown in Fig. 5F, the number of non-lactose-fermenting colonies appeared to increase in the intestinal loops treated with DNase I plus E22 (Fig. 5F, right plate, beige colonies [some marked by arrows]) compared to the plates from an intestinal loop that received E22 alone (Fig. 5F, left plate). Counts of the non-*E. coli* colonies showed a 0.9-log-unit increase in the presence of DNase I but did not reach statistical significance. Surprisingly, most of the non-*E. coli* colonies seen in Fig. 5F, right-hand plate, were *Acinetobacter baumannii*, which is not considered a normal part of the rabbit intestinal microbiota. The results shown in Fig. 5 suggested that extracellular DNA itself may be a powerful regulator of inflammatory responses in the gut, perhaps even rivaling uric acid, despite uric acid's long pedigree as a proinflammatory mediator. In addition, our results suggest that manipulating the formation of DNA NETs *in vivo* may have effects on the microbiota, as well as on enteric pathogens.

To try to account for what was occurring in the intestinal loops, we measured uric acid levels in intestinal loops treated with DNA, DNase I, or both. Figure 6A shows the results obtained in the absence of EPEC or STEC infection. DNase I alone had no effect, but adding 100 μg/ml salmon DNA alone resulted in a near doubling in the uric acid concentration measured after 20 h. Addition of DNA plus DNase I resulted in an even larger increase in uric acid in the intestinal-loop fluid (1,600 μM uric acid is approximately equal to 26.4 mg/dl, or about 4 times the upper limit of normal human serum). Therefore, it appears that DNA may be a source for the generation of uric acid *in vivo* rather than a sink for its removal (for example, by trapping in NETs). Figure 6B shows that uric acid potentiated the release of ATP from HL-60 cells triggered by exposure to hypotonic medium (hypotonic medium was used in Fig. 6B as a surrogate for mechanical deformation, cell stretching, or other stressors leading to ATP release). Figure 6A and B show that uric acid may participate in positive-feedback loops that enhance its own creation (Fig. 6C) (see Discussion).

DISCUSSION

Our study began with our attempt to understand the role of uric acid in EPEC and STEC infections and whether the high levels of uric acid generated *in vivo* (400 to 600 μM) in the gut lumen are "good" or "bad" for the host. Many recent articles have emphasized the role of uric acid as a proinflammatory mediator and its importance in innate immunity (17). If uric acid plays a protective role in the intestine, it might ameliorate some of the deleterious effects of the hydrogen peroxide produced by XO and thereby explain why the XO system continues functioning despite the "uncanny valley" of worsened disease due to the peroxide (3). Our results here show that uric acid does have biological effects independent of hydrogen peroxide and therefore probably plays a protective role at some stage of infection with EPEC and STEC.

Our initial attempts to detect if uric acid could stimulate chemotaxis were disappointing (Fig. 1A to C). Instead, however, uric acid was able to act as a barrier against leukocyte migration (Fig. 1D) and was additive with extracellular DNA in that respect. The results of studies of IL-1β release in response to uric acid were also underwhelming (Fig. 1E). However, uric acid had another biological effect that is much less studied and has not been previously reported, namely, its ability to cause submucosal edema (Fig. 1F and H).

Another novel property of uric acid was its ability to potentiate

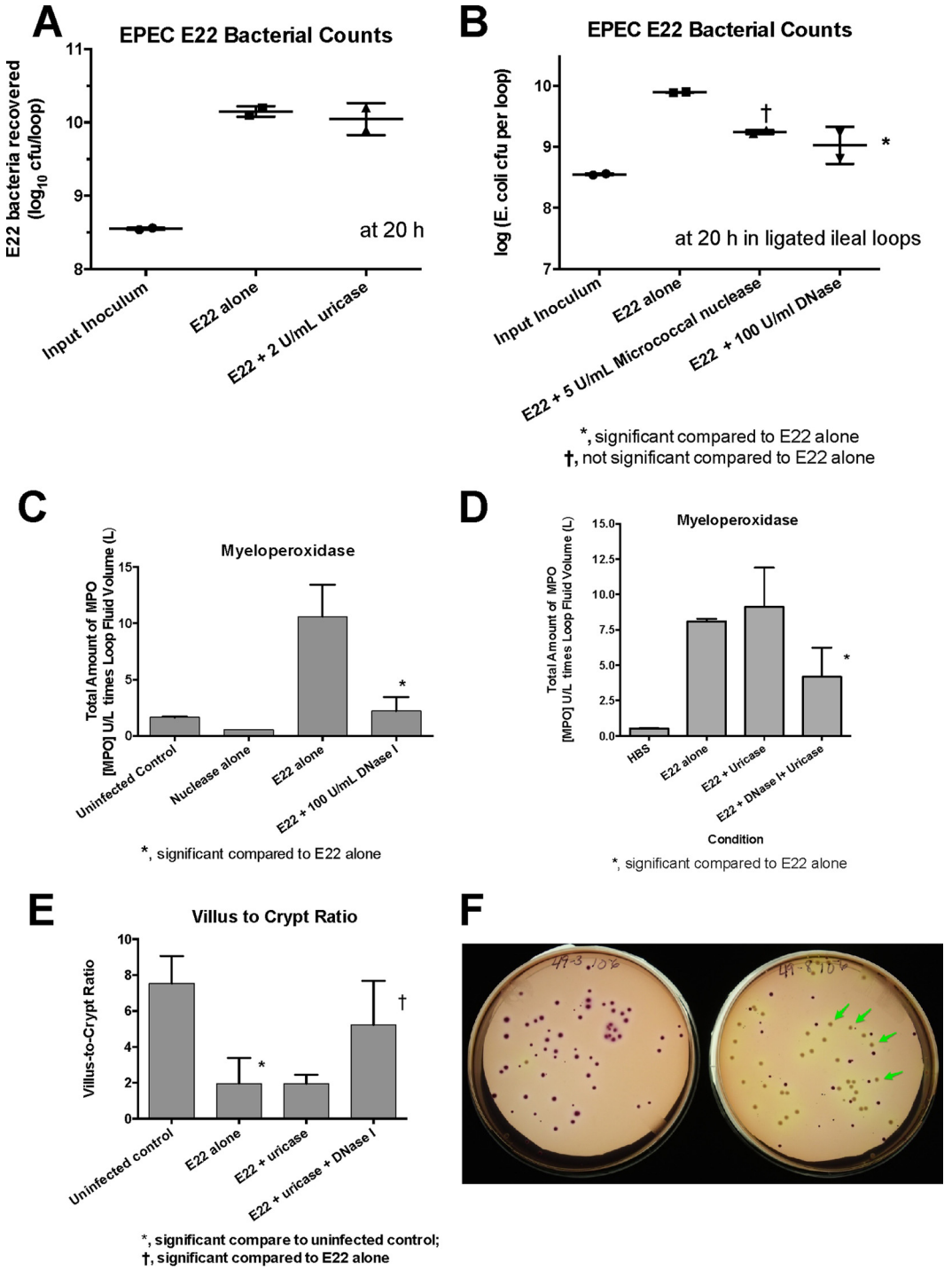

FIG 5 Effects of uricase and DNase I on infection with EPEC E22 in rabbit ileal loops *in vivo*. (A) Lack of effect of uricase on recovery of EPEC E22 bacteria from intestinal loops. (B) Effects of micrococcal nuclease and DNase I on recovery of E22 from rabbit ileal loops. †, micrococcal nuclease just missed statistical significance on E22 bacterial counts. (C) Effect of DNase I on myeloperoxidase activity in the fluid recovered from the ileal loop. (D) Effects of uricase and DNase I on myeloperoxidase in intestinal-loop fluids. (E) Effect of DNase I on histological damage in the ileum, as measured by the villus-to-crypt ratio, an index of villus blunting. (F) Effect of DNase I on the noncoliform aerobic bacteria recovered on MacConkey agar in intestinal loops treated with DNase I (right petri dish; the arrows indicate non-lactose-fermenting colonies) compared to intestinal loops infected with E22 alone (left petri dish; almost all the colonies are coliforms). The error bars indicate SD.

the chloride secretory response triggered by agonists that act via cyclic AMP (Fig. 2), but not by guanylin, which acts via cyclic GMP. To our knowledge, our results are the first to show that uric acid can alter the effects of an intestinal secretagogue in intestinal tissue or any other secretion-competent tissue. Uric acid thus becomes the fourth mediator of secretion that is released into the gut in response to EPEC and STEC infection, the others being ATP (9), adenosine (8), and hydrogen peroxide (3, 14). These enhanc-

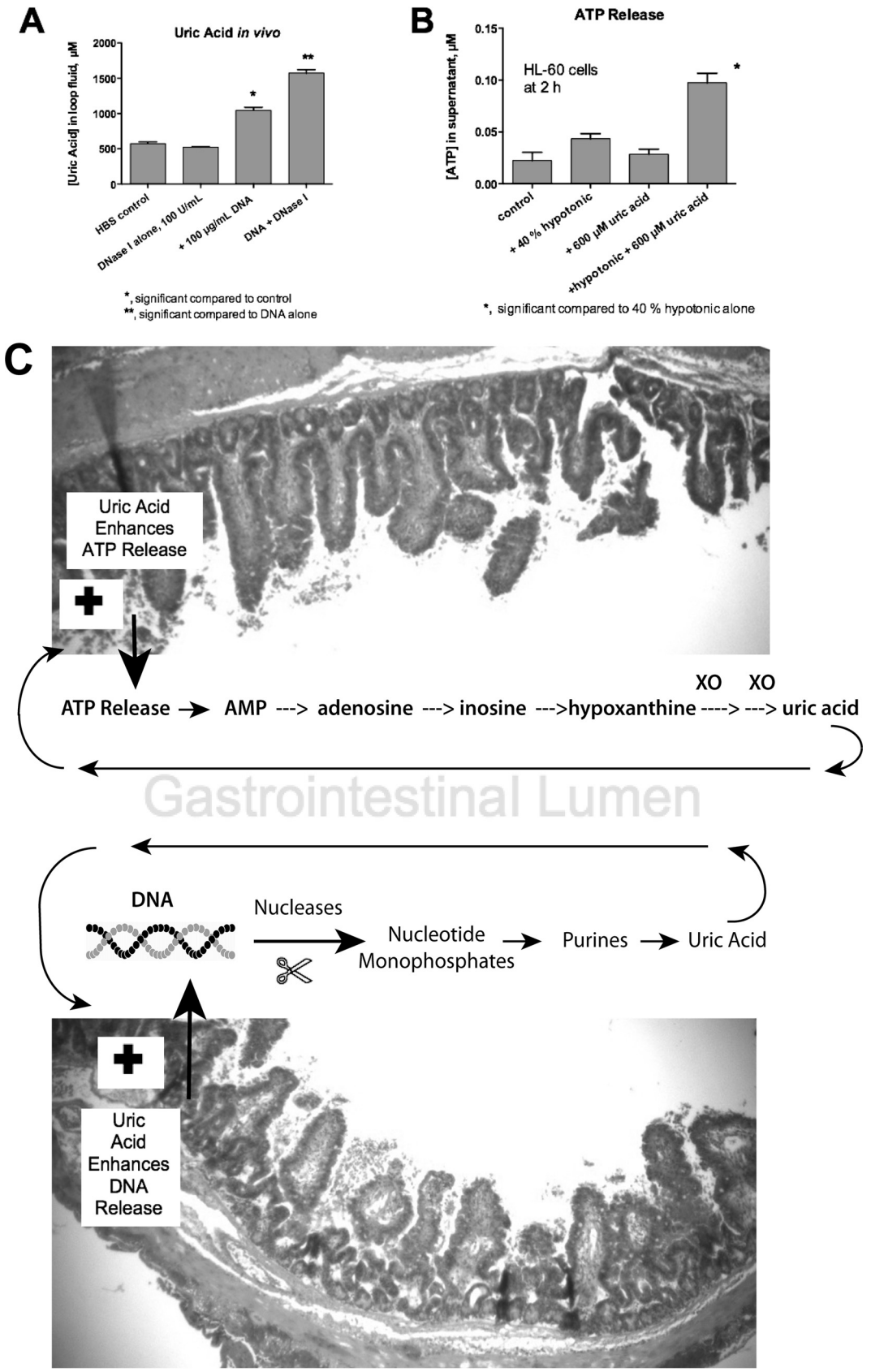

FIG 6 Evidence for positive-feedbacks loops in the intestine. (A) Effect of exogenous DNA with or without DNase I on uric acid formation in the lumen of the rabbit GI tract. Rabbit intestinal loops were left uninfected and were injected with 2 ml of DNase I alone, 2 ml of 100 μg/ml salmon DNA, or DNA plus DNase

ing effects of uric acid on secretion may be relevant to the initial phase of STEC infection, in which watery diarrhea often precedes the onset of bloody diarrhea and hemolytic-uremic syndrome (HUS). It is worth noting that activation of fluid secretion into the gut alters the microbiome (18), even without inflammation or an infectious pathogen. In addition, Fig. 1, 2, 3, and 6 also show that for many biological functions, uric acid acts as a potentiator or enhancer of another stimulus, rather than as the primary trigger.

While other investigators have shown that uric acid can potentiate release of extracellular DNA NETs (15, 19, 20), our results highlight the fact that uric acid itself becomes trapped in the DNA NETs (16). Uric acid crystals appear to be able to form cross-links between different linear DNA strands (Fig. 3A, C, and F). We wonder if uric acid changes the strength or the viscosity of the DNA NETs, but certainly, the uric acid crystals appear to organize the DNA at distances over 100 μm. Most of the DNA NETs reported in the literature have been generated *ex vivo* from neutrophils, eosinophils, or basophils, with a few laboratories going so far as to attempt to visualize NETs in skin or subcutaneous abscesses. Only a few studies have attempted to determine if NETs are formed in internal organs in response to infection (21). We believe we are the first to report the formation of DNA NETs *in vivo* in the intestinal tract.

Since uric acid is reported to have proinflammatory effects (20, 22), as well as being an inducer of NET formation, we expected exogenous uricase to have detectable anti-inflammatory effects *in vivo*, as well. While uricase had antibacterial effects on EPEC bacteria *in vitro* (see Fig. S1 in the supplemental material), its effects *in vivo* were minimal and were eclipsed by those of exogenous DNase I. Unlike uricase, DNase I treatment was accompanied by decreased myeloperoxidase activity, decreased damage to intestinal villi, and decreased recovery of EPEC E22 bacteria from intestinal loops. These findings were the opposite of what one would expect based on the literature on NETs, which emphasizes the role of DNA as an antibacterial host defense (23). Nucleases, which destroy NETs, are supposed to help pathogens survive better (24–26), whereas inhibition of nucleases is supposed to enhance pathogen clearance (27). None of the studies on the role of NETs have been done in the gut, however. The results shown in Fig. 5, therefore, force a reorientation in thinking about whether formation of DNA NETs might actually assist EPEC and STEC in their pathogenic strategies. Extracellular DNA is known to be present in and to strengthen microbial biofilms (28), and EPEC and STEC are strong formers of biofilms (29) (Fig. 4A). Cooper et al. pointed out that selected pathogens, perhaps including EPEC and STEC, can perversely benefit from formation of NETs, rather than being destroyed by them (30). NETs may allow pathogens to remain attached to the mucosa via DNA strands even after damaged enterocytes are sloughed from the epithelium (Fig. 4B and C). Another way that pathogens, including EPEC and STEC, could benefit from DNA NETs is by dining on the nutrients released from damaged host enterocytes, as well as on the DNA itself, for *E. coli* strains are known to be able to take up extracellular DNA and use it as food (31, 32). To quote Finkel and Kolter (31), "DNA is good eating." Adding exogenous DNase to the intestine, as we did in the experiment shown in Fig. 5, may release those nucleotides into the lumen in bulk to the benefit of bystander microbes (Fig. 5F) while depriving the EPEC or STEC bacteria of their meal. Indeed, inhaled DNase (dornase) has been shown to improve outcomes of infection in cystic fibrosis patients (33, 34), and intrapleural injection of DNase plus a fibrinolytic agent improved recovery from empyema of the chest (35). It is very plausible, therefore, that DNA NETs in the gut lumen may assist EPEC and STEC more than they hurt them and that the role of NETs *in vivo* may not be as simple as depicted in studies of neutrophils forming NETs on glass microscope slides.

Figure 6C shows that ATP, which is released into the lumen in response to EPEC and STEC infection (9), can be broken down to uric acid by purine catabolic enzymes naturally present in the gut. However, uric acid, in turn, can trigger even more ATP release (Fig. 6C, top, plus sign), a positive-feedback loop. A similar positive-feedback loop occurs with DNA. EPEC and STEC infections stimulate the formation of extracellular DNA (Fig. 3 and 4), but breakdown of DNA in the gut generates uric acid (Fig. 6A), triggering even more DNA release (Fig. 6C, bottom, plus sign). The two positive-feedback loops shown in Fig. 6C may operate more effectively in the gut than in other tissues because of the presence of digestive enzymes, nucleases, and intestinal nucleotidases that are abundant in the gut but absent or less abundant in other organs. The amount of time needed for the positive-feedback loop to complete its cycle may be several hours, however, explaining why short-term experiments with leukocytes may not adequately model these processes.

The positive-feedback loops shown in Fig. 6C may also explain why EPEC and STEC have such a steep infectious-dose curve, the bane of experimentalists working with animal models. If too low an inoculum of EPEC or STEC is given, there is no "take" of infection and no disease, whereas an inoculum just 1 log unit higher may cause such severe disease that the animals do not survive (J. Crane and Edgar C. Boedeker, personal observations).

Although our work has approached the subject of the role of uric acid from the point of view of basic pathogenesis, uric acid formation in EPEC and STEC infections also seems to be important clinically and diagnostically. Uric acid levels in serum rise above the normal range in several gastrointestinal infections, including rotavirus (36, 37), norovirus (38, 39), and EPEC and STEC (40, 41) infections. Infection with *Salmonella enterica* also triggered a rise in uric acid in cultured T84 cell monolayers (3). Patients with STEC infection may suffer such a severe rise in uric acid levels that uric acid crystals precipitate in the kidney tubules, adding insult to the injury produced by Stx itself (42). Despite this, many clinicians remain unaware of the importance of uric acid

I. After 20 h, the uric acid concentration in the intestinal-loop fluid was assayed, showing that uric acid can be generated *in vivo* in the gut in the presence of DNA. (B) Feedback effects of uric acid on ATP release from HL-60 cells. Uric acid alone did not trigger a release of ATP from HL-60 cells, but it potentiated the ATP release triggered by exposure to hypotonic medium, which causes cell swelling. The hypotonic conditions used here were intended as a surrogate for physical stresses, such as mechanical stimulation, shear stress from liquid flow, or changes in pressure, as may occur *in vivo*. (C) Schematics showing positive-feedback loops that are hypothesized to occur in the GI tract. (Top) ATP released into the lumen as a result of infection is broken down to nucleosides, purines, and uric acid. However, since uric acid can itself enhance ATP release (B), a positive-feedback loop is formed. (Bottom) Uric acid can be formed from the breakdown of DNA, but uric acid also enhances the release of extracellular DNA from host cells (Fig. 3G), so another positive-feedback loop is created. The error bars indicate SD.

metabolism in infectious diarrhea. Clinicians should be encouraged to measure serum uric acid levels in patients with infectious diarrhea, especially if STEC is suspected or confirmed. Two new drugs that can rapidly decrease serum uric acid levels, rasburicase and pegloticase, both recombinant forms of uricase, are available in North America and elsewhere. Even if treatment with these drugs is not contemplated, uric acid levels can provide a clue in diagnosis. For example, hyperuricemia is common in classic HUS due to STEC but rare in atypical HUS, which requires different treatments, such as plasmapheresis or eculizumab. Finally, understanding the role of uric acid in the gut might also allow improvements in the immunogenicity of oral vaccines against enteric infections, such as the oral cholera vaccine, where the degree and duration of protection are still not as strong as desired.

ACKNOWLEDGMENTS

We thank Ashley Jeanlus for her contributions to this project during her summer of research in 2014.

We are thankful to the National Institutes of Health and the National Institute of Allergy and Infectious Diseases (NIAID) for financial support via grant R21 AI 102212.

FUNDING INFORMATION

HHS | National Institutes of Health (NIH) provided funding to John K. Crane under grant number R21 AI 102212.

REFERENCES

1. **Hancock J, Salisbury V, Ovejero-Boglione M, Cherry R, Hoare C, Eisenthal R, Harrison R.** 2002. Antimicrobial properties of milk: dependence on presence of xanthine oxidase and nitrite. Antimicrob Agents Chemother **46:**3308–3310. http://dx.doi.org/10.1128/AAC.46.10.3308-3310.2002.
2. **Yamada Y, Saito H, Tomioka H, Jidoi J.** 1987. Susceptibility of microorganisms to active oxygen species: sensitivity to the xanthine-oxidase-mediated antimicrobial system. J Gen Microbiol **133:**2007–2014.
3. **Crane J, Naeher TM, Broome J, Boedeker E.** 2013. Role of xanthine oxidase in infection due to enteropathogenic and Shiga-toxigenic Escherichia coli. Infect Immun **81:**1129–1139. http://dx.doi.org/10.1128/IAI.01124-12.
4. **Behrens MD, Wagner WM, Krco CJ, Erskine CL, Kalli KR, Krempski J, Gad EA, Disis ML, Knutson KL.** 2008. The endogenous danger signal, crystalline uric acid, signals for enhanced antibody immunity. Blood **111:**1472–1479.
5. **Martinon F, Petrilli V, Mayor A, Tardivel A, Tschopp J.** 2006. Gout-associated uric acid crystals activate the NALP3 inflammasome. Nature **440:**237–241. http://dx.doi.org/10.1038/nature04516.
6. **Crane JK, Mongiardo KM.** 2014. Pro-inflammatory effects of uric acid in the gastrointestinal tract. Immunol Invest **43:**255–266. http://dx.doi.org/10.3109/08820139.2013.864667.
7. **Tait AR, Davidson BA, Johnson KJ, Remick DG, Knight PR.** 1993. Halothane inhibits the intraalveolar recruitment of neutrophils, lymphocytes, and macrophages in response to influenza virus infection in mice. Anesthesia Analgesia **76:**1106–1113.
8. **Crane JK, Shulgina I, Naeher TM.** 2007. Ecto-5′-nucleotidase and intestinal ion secretion by enteropathogenic Escherichia coli. Purinergic Signal **3:**233–246. http://dx.doi.org/10.1007/s11302-007-9056-0.
9. **Crane J, Olson R, Jones H, Duffey M.** 2002. Release of ATP during host cell killing by enteropathogenic E. coli and its role as a secretory mediator. Am J Physiol Gastrointest Liver Physiol **283:**G74–G86. http://dx.doi.org/10.1152/ajpgi.00484.2001.
10. **Petrilli V, Dostert C, Muruve DA, Tschopp J.** 2007. The inflammasome: a danger sensing complex triggering innate immunity. Curr Opin Immunol **19:**615–622. http://dx.doi.org/10.1016/j.coi.2007.09.002.
11. **Di Giovine FS, Malawista SE, Nuki G, Duff GW.** 1987. Interleukin 1 (IL 1) as a mediator of crystal arthritis. Stimulation of T cell and synovial fibroblast mitogenesis by urate crystal-induced IL 1. J Immunol **138:**3213–3218.
12. **Richardson SE, Karmali MA, Becker LE, Smith CR.** 1988. The histopathology of the hemolytic uremic syndrome associated with verocytotoxin-producing Escherichia coli infections. Hum Pathol **19:**1102–1108. http://dx.doi.org/10.1016/S0046-8177(88)80093-5.
13. **Mallick EM, McBee ME, Vanguri VK, Melton-Celsa AR, Schlieper K, Karalius BJ, O'Brien AD, Butterton JR, Leong JM, Schauer DB.** 2012. A novel murine infection model for Shiga toxin-producing Escherichia coli. J Clin Invest **122:**4012–4024. http://dx.doi.org/10.1172/JCI62746.
14. **Nguyen TD, Canada AT.** 1994. Modulation of human colonic T84 cell secretion by hydrogen peroxide. Biochem Pharmacol **47:**403–410. http://dx.doi.org/10.1016/0006-2952(94)90032-9.
15. **Schorn C, Janko C, Latzko M, Chaurio R, Schett G, Herrmann M.** 2012. Monosodium urate crystals induce extracellular DNA traps in neutrophils, eosinophils, and basophils but not in mononuclear cells. Front Immunol **3:**277. http://dx.doi.org/10.3389/fimmu.2012.00277.
16. **Schorn C, Janko C, Krenn V, Zhao Y, Munoz LE, Schett G, Herrmann M.** 2012. Bonding the foe—NETting neutrophils immobilize the pro-inflammatory monosodium urate crystals. Front Immunol **3:**376. http://dx.doi.org/10.3389/fimmu.2012.00376.
17. **Shi Y, Mucsi AD, Ng G.** 2010. Monosodium urate crystals in inflammation and immunity. Immunol Rev **233:**203–217. http://dx.doi.org/10.1111/j.0105-2896.2009.00851.x.
18. **Keely S, Kelly CJ, Weissmueller T, Burgess A, Wagner BD, Robertson CE, Harris JK, Colgan SP.** 2012. Activated fluid transport regulates bacterial-epithelial interactions and significantly shifts the murine colonic microbiome. Gut Microbes **3:**250–260. http://dx.doi.org/10.4161/gmic.20529.
19. **Arai Y, Nishinaka Y, Arai T, Morita M, Mizugishi K, Adachi S, Takaori-Kondo A, Watanabe T, Yamashita K.** 2014. Uric acid induces NADPH oxidase-independent neutrophil extracellular trap formation. Biochem Biophys Res Commun **443:**556–561. http://dx.doi.org/10.1016/j.bbrc.2013.12.007.
20. **Mitroulis I, Kambas K, Chrysanthopoulou A, Skendros P, Apostolidou E, Kourtzelis I, Drosos GI, Boumpas DT, Ritis K.** 2011. Neutrophil extracellular trap formation is associated with IL-1beta and autophagy-related signaling in gout. PLoS One **6:**e29318. http://dx.doi.org/10.1371/journal.pone.0029318.
21. **Rohm M, Grimm MJ, D'Auria AC, Almyroudis NG, Segal BH, Urban CF.** 2014. NADPH oxidase promotes neutrophil extracellular trap formation in pulmonary aspergillosis. Infect Immun **82:**1766–1777. http://dx.doi.org/10.1128/IAI.00096-14.
22. **Kahlenberg JM, Carmona-Rivera C, Smith CK, Kaplan MJ.** 2013. Neutrophil extracellular trap-associated protein activation of the NLRP3 inflammasome is enhanced in lupus macrophages. J Immunol **190:**1217–1226. http://dx.doi.org/10.4049/jimmunol.1202388.
23. **Brinkmann V, Reichard U, Goosmann C, Fauler B, Uhlemann Y, Weiss DS, Weinrauch Y, Zychlinsky A.** 2004. Neutrophil extracellular traps kill bacteria. Science **303:**1532–1535. http://dx.doi.org/10.1126/science.1092385.
24. **Munafo DB, Johnson JL, Brzezinska AA, Ellis BA, Wood MR, Catz SD.** 2009. DNase I inhibits a late phase of reactive oxygen species production in neutrophils. J Innate Immun **1:**527–542. http://dx.doi.org/10.1159/000235860.
25. **Derre-Bobillot A, Cortes-Perez NG, Yamamoto Y, Kharrat P, Couve E, Da Cunha V, Decker P, Boissier MC, Escartin F, Cesselin B, Langella P, Bermudez-Humaran LG, Gaudu P.** 2013. Nuclease A (Gbs0661), an extracellular nuclease of Streptococcus agalactiae, attacks the neutrophil extracellular traps and is needed for full virulence. Mol Microbiol **89:**518–531. http://dx.doi.org/10.1111/mmi.12295.
26. **Morita C, Sumioka R, Nakata M, Okahashi N, Wada S, Yamashiro T, Hayashi M, Hamada S, Sumitomo T, Kawabata S.** 2014. Cell wall-anchored nuclease of Streptococcus sanguinis contributes to escape from neutrophil extracellular trap-mediated bacteriocidal activity. PLoS One **9:**e103125. http://dx.doi.org/10.1371/journal.pone.0103125.
27. **Schilcher K, Andreoni F, Uchiyama S, Ogawa T, Schuepbach RA, Zinkernagel AS.** 2014. Increased neutrophil extracellular trap-mediated Staphylococcus aureus clearance through inhibition of nuclease activity by clindamycin and immunoglobulin. J Infect Dis **210:**473–482. http://dx.doi.org/10.1093/infdis/jiu091.
28. **Bass JIF, Russo DM, Gabelloni ML, Geffner JR, Giordano M, Catalano M, Zorreguieta Á Trevani AS.** 2010. Extracellular DNA: a major proinflammatory component of Pseudomonas aeruginosa biofilms. J Immunol **184:**6386–6395. http://dx.doi.org/10.4049/jimmunol.0901640.
29. **Moreira CG, Palmer K, Whiteley M, Sircili MP, Trabulsi LR, Castro AF,**

Sperandio V. 2006. Bundle-forming pili and EspA are involved in biofilm formation by enteropathogenic Escherichia coli. J Bacteriol **188:**3952–3961. http://dx.doi.org/10.1128/JB.00177-06.
30. **Cooper PR, Palmer LJ, Chapple IL.** 2013. Neutrophil extracellular traps as a new paradigm in innate immunity: friend or foe? Periodontology 2000 **63:**165–197. http://dx.doi.org/10.1111/prd.12025.
31. **Finkel SE, Kolter R.** 2001. DNA as a nutrient: novel role for bacterial competence gene homologs. J Bacteriol **183:**6288–6293. http://dx.doi.org/10.1128/JB.183.21.6288-6293.2001.
32. **Palchevskiy V, Finkel SE.** 2006. Escherichia coli competence gene homologs are essential for competitive fitness and the use of DNA as a nutrient. J Bacteriol **188:**3902–3910. http://dx.doi.org/10.1128/JB.01974-05.
33. **Quan JM, Tiddens HA, Sy JP, McKenzie SG, Montgomery MD, Robinson PJ, Wohl MEB, Konstan MW, Pulmozyme Early Intervention Trial Study Group.** 2001. A two-year randomized, placebo-controlled trial of dornase alfa in young patients with cystic fibrosis with mild lung function abnormalities. J Pediatr **139:**813–820. http://dx.doi.org/10.1067/mpd.2001.118570.
34. **Flume PA, O'Sullivan BP, Robinson KA, Goss CH, Mogayzel PJ, Jr, Willey-Courand DB, Bujan J, Finder J, Lester M, Quittell L.** 2007. Cystic fibrosis pulmonary guidelines: chronic medications for maintenance of lung health. Am J Respir Crit Care Med **176:**957–969. http://dx.doi.org/10.1164/rccm.200705-664OC.
35. **Rahman NM, Maskell NA, West A, Teoh R, Arnold A, Mackinlay C, Peckham D, Davies CWH, Ali N, Kinnear W, Bentley A, Kahan BC, Wrightson JM, Davies HE, Hooper CE, Lee YCG, Hedley EL, Crosthwaite N, Choo L, Helm EJ, Gleeson FV, Nunn AJ, Davies RJO.** 2011. Intrapleural use of tissue plasminogen activator and DNase in pleural infection. N Engl J Med **365:**518–526. http://dx.doi.org/10.1056/NEJMoa1012740.
36. **Palla G, Ughi C, Villirillo A, Cesaretti G, Maggiore G, Ventura A.** 1996. Serum uric acid elevations in viral enteritis. Pediatr Infect Dis J **15:**642–643.
37. **Palla G, Ughi C, Cesaretti G, Ventura A, Maggiore G.** 1997. "Automatic" diagnosis of viral enteritis. J Pediatr **130:**1013–1014.
38. **Ashida A, Shirasu A, Nakakura H, Tamai H.** 2010. Acute renal failure due to obstructive urate stones associated with norovirus gastroenteritis. Pediatr Nephrol **25:**2377–2378. http://dx.doi.org/10.1007/s00467-010-1607-x.
39. **Morita T, Fujieda M.** 2011. Acidosis with hyperuricemia and renal tubular damage in viral gastroenteritis. Pediatr Nephrol **26:**2259–2260. http://dx.doi.org/10.1007/s00467-011-2003-x.
40. **Balestracci A, Martin SM, Toledo I.** 2012. Hyperuricemia in children with post-diarrheal hemolytic uremic syndrome. Pediatr Nephrol **27:**1421–1422. http://dx.doi.org/10.1007/s00467-012-2181-1.
41. **Kaplan B, Thomson P.** 1976. Hyperuricemia in the hemolytic-uremic syndrome. Am J Dis Child **130:**854–856.
42. **O'Regan S, Rousseau E.** 1988. Hemolytic uremic syndrome: urate nephropathy superimposed on an acute glomerulopathy? An hypothesis. Clin Nephrol **30:**207–201.
43. **Levine M, Nalin D, Hornick R, Bergquist E, Waterman D, Young C, Sotman S, Rowe B.** 1978. Escherichia coli strains that cause diarrhea but do not produce heat-labile or heat-stable enterotoxins and are not invasive. Lancet **i:**1119–1122.
44. **Levine M, Nataro J, Karch H, Baldini M, Kaper J, Black R, Clements M, O'Brien A.** 1985. The diarrheal response of humans to some classic serotypes of enteropathogenic Escherichia coli is dependent on a plasmid encoding an enteroadhesiveness factor. J Infect Dis **152:**550–559. http://dx.doi.org/10.1093/infdis/152.3.550.
45. **Milon A, Oswald E, De Rycke J.** 1999. Rabbit EPEC: a model for the study of enteropathogenic *Escherichia coli*. Vet Res **30:**203–219.
46. **Zhu C, Yu J, Yang Z, Davis K, Rios H, Wang B, Glenn G, Boedeker EC.** 2008. Protection against Shiga toxin-producing Escherichia coli infection by transcutaneous immunization with Shiga toxin subunit B. Clin Vaccine Immunol **15:**359–366. http://dx.doi.org/10.1128/CVI.00399-07.
47. **Agin TS, Zhu C, Johnson LA, Thate TE, Yang Z, Boedeker EC.** 2005. Protection against hemorrhagic colitis in an animal model by oral immunization with isogeneic rabbit enteropathogenic Escherichia coli attenuated by truncating intimin. Infect Immun **73:**6608–6619. http://dx.doi.org/10.1128/IAI.73.10.6608-6619.2005.